

Solid Mercury Dihydride: Mercurophilic Bonding in Molecular HgH<sub>2</sub> Polymers

Xuefeng Wang and Lester Andrews\*

Department of Chemistry, University of Virginia, P.O. Box 400319,  
Charlottesville, Virginia 22904-4319

Received July 8, 2004

Atomic mercury subjected to mercury arc irradiation reacts in solid hydrogen to give the linear HgH<sub>2</sub> molecule with strong IR absorptions at 1902 and 773 cm<sup>-1</sup>. Annealing leads to HgH<sub>2</sub> dimer and trimer, and warming above 7 K allows the hydrogen matrix to sublime and solid HgH<sub>2</sub> to form. This covalent molecular solid is characterized by strong IR absorptions at 1802 and 673 cm<sup>-1</sup> and by decomposition at 150–170 K.

## Introduction

Mercury is a curious element. Mercury is the only liquid metal at room temperature, it is unreactive owing to its closed-shell electron configuration, but many of its compounds are extremely toxic. For example, mercury reacts slowly with chlorine to form HgCl<sub>2</sub>, a poisonous compound, but it reacts with hydrogen only when excited by ultraviolet light or electrical discharge.<sup>1–6</sup> Thus, mercury hydrides are limited to HgH<sup>+</sup> and HgH in electrical discharges and photoexcitation of the Hg–H<sub>2</sub> complex in a supersonic jet<sup>7,8</sup> and HgH<sub>2</sub> formed in the reaction of H<sub>2</sub> and Hg excited by 249 nm laser irradiation in solid matrix samples at very low temperatures.<sup>4,5</sup> There are no stable mercury hydride compounds although an unstable mercury hydride is probably formed when HgI<sub>2</sub> and LiAlH<sub>4</sub> react at –135 °C: the white solid product decomposed above –125 °C, and no spectroscopic measurements were made.<sup>9</sup>

Recently, laser-ablated Al atoms were reacted with pure hydrogen during condensation at 3.5 K to form AlH, and subsequent ultraviolet irradiation produced AlH<sub>3</sub> and its dimer, the elusive Al<sub>2</sub>H<sub>6</sub> molecule.<sup>10</sup> Warming above 7 K

allowed the H<sub>2</sub> matrix host to evaporate and solid AlH<sub>3</sub> to form on the cold window. Similar experiments with In and hydrogen gave indium hydrides, the even more elusive In<sub>2</sub>H<sub>6</sub> molecule, and finally solid indane.<sup>11</sup> Here we irradiate samples of Hg in solid hydrogen at 4.5 K with a common mercury arc street lamp to form HgH<sub>2</sub>. Next we warm the sample to 5–7 K to allow diffusion and molecular association: thus, (HgH<sub>2</sub>)<sub>2</sub> dimer and (HgH<sub>2</sub>)<sub>3</sub> trimer are formed sequentially. The solid H<sub>2</sub> host sublimates away on warming above 7 K, but a solid molecular mercury hydride polymer (HgH<sub>2</sub>)<sub>n</sub> remains on the cold window until it decomposes in the 150–170 K temperature range. Accordingly, we report here the first infrared spectrum and characterization of solid mercury hydride.

## Experimental Methods

Mercury was evaporated at 50–55 °C through a stainless steel valve (Nupro SS4BK) and tube into a hydrogen stream condensing on a CsI window at 4.5 K.<sup>12</sup> A 2 m mole amount of H<sub>2</sub> gas was codeposited with Hg vapor for 20 min. The Hg/H<sub>2</sub> samples were subjected to ultraviolet irradiation using a mercury arc lamp (Sylvania H39 KB-175, outer globe removed), and infrared spectra were recorded on a Nicolet 750 instrument at 0.5 cm<sup>-1</sup> resolution and 0.1 cm<sup>-1</sup> frequency accuracy. Samples were annealed using resistance heat, the refrigerator was switched off, and infrared spectra were recorded as the cold window warmed to room temperature.

## Results and Discussion

Infrared spectra from an experiment with mercury and solid hydrogen are illustrated in Figure 1. No new absorption was observed on codeposition as ground-state mercury does not react with hydrogen.<sup>4</sup> Solid hydrogen absorptions were

\* To whom correspondence should be addressed. E-mail: isa@virginia.edu.

- (1) Cotton, F. A.; Wilkinson, G.; Murillo, C. A.; Bochmann, M. *Advanced Inorganic Chemistry*, 6th ed.; Wiley: New York, 1999.
- (2) Greenwood, N. N.; Earnshaw, A. *Chemistry for the Elements*; Pergamon: Oxford, U.K., 1984; p 125.
- (3) O'Neil, M. J.; Smith, A.; Heckelman, P. E. *The Merck Index*, 13th ed.; Merck: Englewood Cliffs, NJ, 2001; pp 1050–1053.
- (4) Legay-Sommaire, N.; Legay, F. *Chem. Phys. Lett.* **1993**, *207*, 123.
- (5) Legay-Sommaire, N.; Legay, F. *J. Phys. Chem.* **1995**, *99*, 16945.
- (6) Greene, T. M.; Brown, E.; Andrews, L.; Downs, A. J.; Chertihin, G. V.; Runeberg, N.; Pyykkö, P. *J. Phys. Chem.* **1995**, *99*, 7925 and references therein.
- (7) Huber, K. P.; Herzberg, G. *Constants of Diatomic Molecules*; Van Nostrand: Princeton, NJ, 1979.
- (8) Breckenridge, W. H.; Jouvet, C.; Soep, B. *J. Chem. Phys.* **1986**, *84*, 1443.
- (9) Wiberg, E.; Henle, W. *Z. Naturforsch.* **1951**, *6b*, 461 (Hg).

(10) Andrews, L.; Wang, X. *Science* **2003**, *299*, 2049.

(11) Andrews, L.; Wang, X. *Angew. Chem., Int. Ed.* **2004**, *43*, 1706.

(12) Andrews, L. *Chem. Soc. Rev.* **2004**, *33*, 123.

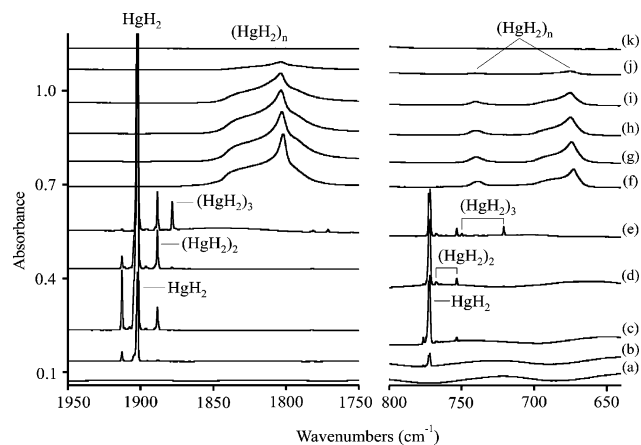


**Figure 1.** Infrared spectra in the 1950–1750 and 800–640  $\text{cm}^{-1}$  regions for mercury atoms in solid hydrogen at 4.5 K: (a) spectrum after 2 mmol of  $\text{H}_2$  codeposited with Hg vapor from 50 to 55  $^\circ\text{C}$  liquid; (b) after irradiation at 240–380 nm for 25 min; (c) after irradiation at  $\lambda > 220$  nm for 15 min; (d) after annealing to 6.0 K and cooling back to 4.5 K; (e) after annealing to 7.0 K; (f) after annealing to 7.5 K; (g) spectrum at 110–130 K; (h) spectrum at 140–150 K; (i) spectrum at 150–160 K; (j) spectrum at 160–165 K; (k) spectrum at 165–170 K.

observed in the region above 4100  $\text{cm}^{-1}$ .<sup>13,14</sup> Irradiation at 240–380 nm (black filter) produces strong new bands at 1902.3 and 772.8  $\text{cm}^{-1}$ , which are in excellent agreement with the 1902.7 and 772.5  $\text{cm}^{-1}$  bands observed for  $\text{HgH}_2$  after 249 nm laser irradiation of solid hydrogen at 5.7 K,<sup>4</sup> plus new weaker bands at 1912.9, 1886.6, and 753.4  $\text{cm}^{-1}$ . Irradiation with the full light ( $\lambda > 220$  nm) of the mercury arc markedly increased these absorptions and produced a weak band at 1205.6  $\text{cm}^{-1}$  (not shown) for  $\text{HgH}$  diatomic.<sup>4,7,8</sup> Next the sample was annealed to 6.0, 7.0, and 7.5 K, and the spectra in Figure 1 show several noteworthy changes. The 1912.9  $\text{cm}^{-1}$  absorption is virtually destroyed, the 1902.3 and 772.8  $\text{cm}^{-1}$  bands decrease slightly, the 1886.6 and 753.4  $\text{cm}^{-1}$  bands increase, the 1878.3 and 720.9  $\text{cm}^{-1}$  bands increase last, a broad new band at 1880–1800  $\text{cm}^{-1}$  and sharp absorption at 1771.3  $\text{cm}^{-1}$  appear in the upper region, and new features at 749.7 and 720.9  $\text{cm}^{-1}$  come in the lower region. On annealing of the sample to 7.5 K, all of the above sharp product bands and absorptions due to solid hydrogen disappear and broader absorptions appear at 1836, 1802.0, 739.1, and 672.9  $\text{cm}^{-1}$ . These latter bands remain in spectra recorded on the cold window up to 140–150 K, and they disappear in the 150–165 K range. Thus, the absorptions are gone after the cold window reaches 170 K. The same results were obtained in another experiment run under the same conditions.

Infrared spectra from analogous investigations with Hg and  $\text{D}_2$  are shown in Figure 2, and the absorption positions are given in Table 1. The photochemical and sample warming behaviors are the same as found for hydrogen except that broad bands formed between 10 and 30 K then give way to sharper features in the 80–140 K range.

Several experiments were done with pure HD, and the major product absorptions were observed at 1956.5, 1398.6,

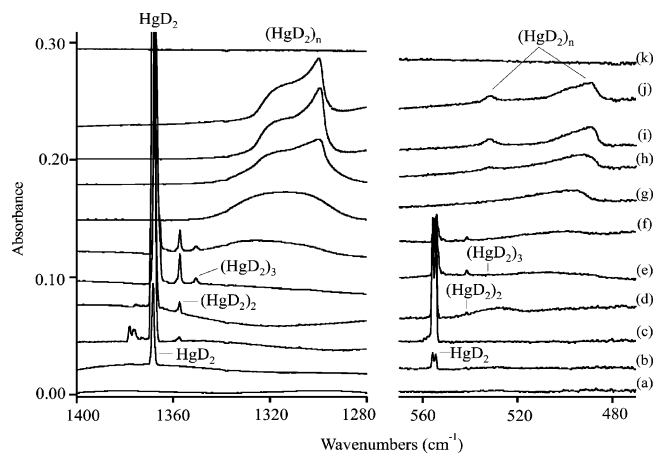


**Figure 2.** Infrared spectra in the 1400–1280 and 570–470  $\text{cm}^{-1}$  regions for mercury atoms in solid deuterium at 4.5 K: (a) spectrum after 2 mmol of  $\text{D}_2$  codeposited with Hg vapor from 50 to 55  $^\circ\text{C}$  liquid; (b) after irradiation at 240–380 nm for 25 min; (c) after irradiation at  $\lambda > 220$  nm for 15 min; (d) after annealing to 7.5 K and cooling back to 4.5 K; (e) after annealing to 10 K; (f) after annealing to 11 K; (g) spectrum at 30–70 K; (h) spectrum at 80–110 K; (i) spectrum at 120–140 K; (j) spectrum at 160–170 K; (k) spectrum at 170–175 K.

**Table 1.** Infrared Absorptions ( $\text{cm}^{-1}$ ) Observed for Mercury Hydrides in Solid Hydrogen or Deuterium

$\text{H}_2$	$\text{D}_2$	hydride
4142.5	2980.7	$\text{HgH}_2(\text{H}_2)_n$
4137.6	2977.4	$\text{HgH}_2(\text{H}_2)_n$
1912.9	1378.0	(X) $\text{HgH}_2^a$
1902.3	1368.4	$\text{HgH}_2$ ( $\nu_3$ , str)
1886.6	1357.3	$(\text{HgH}_2)_2$
1878.3	1350.5	$(\text{HgH}_2)_3$
1836 sh	1320 sh	$(\text{HgH}_2)_n$
1802.0	1299.7	$(\text{HgH}_2)_n$
1771.3	1272.5	HHgHgH
1205.6	899.8	HgH
772.8	555.9	$\text{HgH}_2$ ( $\nu_2$ , bend)
764.3		$(\text{HgH}_2)_2$
753.4	541.6	$(\text{HgH}_2)_2$
749.7		$(\text{HgH}_2)_3$
720.9	517.2	$(\text{HgH}_2)_3$
739.1	531.8	$(\text{HgH}_2)_n$
672.9	488.9	$(\text{HgH}_2)_n$

<sup>a</sup>  $\text{HgH}_2$  in a more open matrix site or perhaps perturbed by unreacted Hg.

and 676.1  $\text{cm}^{-1}$  for HHgD with weaker bands at 1905.2 and 1369.9  $\text{cm}^{-1}$  for  $\text{HgH}_2$  and  $\text{HgD}_2$ , respectively. These bands are shown in Figure 3 for the Hg–H and Hg–D stretching regions. Note that the latter fundamentals are slightly different in pure HD. In addition weak HgH and HgD bands are observed at 1207.0 and 898.5  $\text{cm}^{-1}$ . Warming to evaporate the HD host formed new broader 1874 and 1339  $\text{cm}^{-1}$  bands and new sharper 1819 and 1308  $\text{cm}^{-1}$  absorptions, which are displayed in Figure 3. A parallel investigation with 50/50  $\text{H}_2/\text{D}_2$  gave strong 1902.6 and 1368.1 and weaker 1955.5 and 1397.9  $\text{cm}^{-1}$  absorptions just the reverse found with pure HD. Sample warming to evaporate the  $\text{H}_2/\text{D}_2$  host produced sharper bands at 1875 and 1341  $\text{cm}^{-1}$  and broader bands at 1813 and 1308  $\text{cm}^{-1}$ .

The strong 1902.3 and 772.8  $\text{cm}^{-1}$  absorptions are clearly due to the linear HHgH molecule as identified by the Legays<sup>4,5</sup> and supported by theoretical calculations including vibrational frequencies.<sup>6,15–18</sup> The Hg +  $\text{H}_2$  reaction is

(13) Gush, H. P.; Hare, W. F.; Allin, E. J.; Welsh, H. L. *Can. J. Phys.* **1960**, *38*, 176.

(14) Andrews, L.; Wang, X. *J. Phys. Chem. A* **2004**, *108*, 3879.

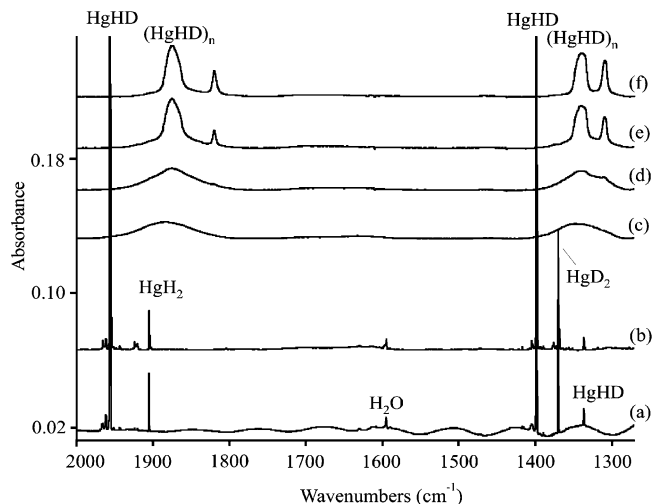
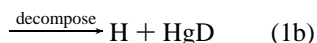
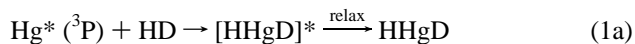


**Figure 3.** Infrared spectrum in the 2000–1270  $\text{cm}^{-1}$  region for mercury atoms in solid HD at 4.5 K: (a) spectrum after 2 mmol of HD codeposited with Hg vapor from 50 to 55 °C liquid and after irradiation at  $\lambda > 220$  nm for 25 min; (b) after annealing to 9.0 K and cooling back to 4.5 K; (c) after annealing to 10.2 K; (d) spectrum at 65–100 K; (e) spectrum at 105–135 K; (f) spectrum at 140–150 K.

endothermic, and excitation of Hg is required to initiate the reaction.<sup>6,16,17</sup> Associated absorptions are observed in the H–H stretching region at 4142.5 and 4137.6  $\text{cm}^{-1}$ ; hence, the HHgH molecule here is complexed weakly by dihydrogen molecules. The deuterium counterparts at 1368.4 and 555.9  $\text{cm}^{-1}$  for DHgD define H/D frequency ratios of 1.3901 and 1.3902 that are appropriate for heavy metal–hydrogen stretching and bending vibrations, and both H–H complex modes exhibit D–D counterparts and the H/D ratio 1.3897 that is common for H–H stretching modes.<sup>12,14</sup> Our pure HD experiment forms HHgD with strong absorptions at 1956.5, 1398.6, and 676.1  $\text{cm}^{-1}$  and weak HD complex band at 3617.5  $\text{cm}^{-1}$ . In addition very much weaker bands are observed for HgH<sub>2</sub> and HgD<sub>2</sub>. This means that the primary insertion product HHgD is for the most part relaxed and stabilized by the solid HD matrix, reaction (1a), but a very small fraction decomposes to HgH or HgD, reactions (1b) and (1c). A small amount of isotopic scrambling can then take place when the H atom from (1b) finds the HgH product of (1c) and D from (1c) combines with HgD from (1b). Reaction (1a) requires excitation of Hg to the <sup>3</sup>P state,<sup>4–6,8,18</sup> and the mercury arc lamp provides a perfect source to make a very high primary product yield.



The bands at 1888.6 and 1878.3  $\text{cm}^{-1}$  increase on annealing at different rates: the latter is favored at the expense of the former on annealing to 7.5 K (Figure 1e). Analogous bands at 1933.7 and 1920.4  $\text{cm}^{-1}$  in solid nitrogen

(15) Pyykkö, P. *J. Chem. Soc., Faraday Trans. 2* **1979**, 75, 1256.

(16) Schwerdtfeger, P.; Heath, G. A.; Dolg, M.; Bennett, M. A. *J. Am. Chem. Soc.* **1992**, 114, 7518.

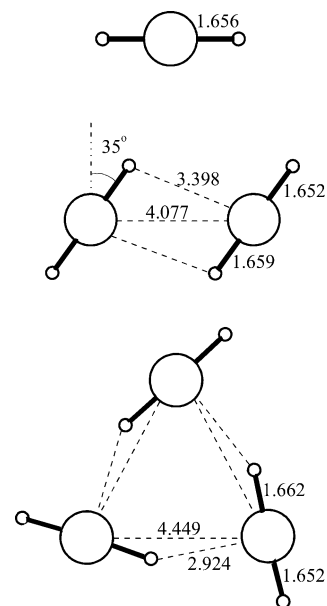


**Figure 4.** Structures computed for  $(\text{HgH}_2)_n$  ( $n = 1-3$ ) molecular clusters at the B3LYP/6-311++G(3df,3pd)/SDD level. Distances are in Å, and angles are in deg.

were assigned to the van der Waals dimer  $(\text{HgH}_2)_2$ .<sup>5</sup> We agree on the assignment of the first band to grow on annealing as dimer, but we reassign the band favored at higher temperature to trimer. Associated bands at 764.3 (weak) and 753.4  $\text{cm}^{-1}$  (strong) are also assigned to the dimer and at 749.7 (weak) and 720.9  $\text{cm}^{-1}$  (strong) to the trimer in the bending mode region.

Pyykkö and Straka have addressed metallophilic attraction in  $(\text{HgH}_2)_2$  dimers as a special case of closed-shell interactions.<sup>19,20</sup> These workers performed MP2 calculations for four dimer structures but did not report frequencies. We need a consistent set of frequencies for  $(\text{HgH}_2)_n$  ( $n = 1-4$ ) so we calculate structures and frequencies at the B3LYP level using the 6-311++G(3df,3pd) basis set and SDD pseudopotential.<sup>21</sup> (Our MP2 calculations give slightly shorter van der Waals distances and higher frequencies.) Figure 4 shows the structures we obtained, and Table 2 gives the calculated frequencies. Note our optimized dimer has a strong Hg–H stretching fundamental 5.5  $\text{cm}^{-1}$  below HHgH, we observe a 13.7  $\text{cm}^{-1}$  difference, our trimer calculation predicts the

(17) Schwerdtfeger, P.; Boyd, D. W.; Brienne, S.; McFeaters, J. S.; Dolg, M.; Liao, M.-S.; Eugen Schwarz, W. H. *Inorg. Chim. Acta* **1993**, 213, 233.

(18) Bernier, A.; Millie, P. *J. Chem. Phys.* **1988**, 88, 4843.

(19) Pyykkö, P.; Straka, M. *Phys. Chem. Chem. Phys.* **2000**, 2, 2489.

(20) Pyykkö, P. *Chem. Rev.* **1997**, 97, 597.

(21) Frisch, M. J.; Trucks, G. W.; Schlegel, H. B.; Scuseria, G. E.; Robb, M. A.; Cheeseman, J. R.; Zakrzewski, V. G.; Montgomery, J. A., Jr.; Stratmann, R. E.; Burant, J. C.; Dapprich, S.; Millam, J. M.; Daniels, A. D.; Kudin, K. N.; Strain, M. C.; Farkas, O.; Tomasi, J.; Barone, V.; Cossi, M.; Cammi, R.; Mennucci, B.; Pomelli, C.; Adamo, C.; Clifford, S.; Ochterski, J.; Petersson, G. A.; Ayala, P. Y.; Cui, Q.; Morokuma, K.; Malick, D. K.; Rabuck, A. D.; Raghavachari, K.; Foresman, J. B.; Cioslowski, J.; Ortiz, J. V.; Stefanov, B. B.; Liu, G.; Liashenko, A.; Piskorz, P.; Komaromi, I.; Gomperts, R.; Martin, R. L.; Fox, D. J.; Keith, T.; Al-Laham, M. A.; Peng, C. Y.; Nanayakkara, A.; Gonzalez, C.; Challacombe, M.; Gill, P. M. W.; Johnson, B.; Chen, W.; Wong, M. W.; Andres, J. L.; Gonzalez, C.; Head-Gordon, M.; Replogle, E. S.; Pople, J. A. *Gaussian 98*, revision A.11.4; Gaussian, Inc.: Pittsburgh, PA, 1998; and references therein.

**Table 2.** Frequencies ( $\text{cm}^{-1}$ ) Calculated for  $\text{HgH}_2$  and Several Molecular Clusters

	Hg–H str	H–Hg–H bend
$\text{HgH}_2$	1923 (472) <sup>a,b</sup>	793 (33 × 2) <sup>a,b</sup>
$(\text{HgH}_2)_2$	1918 (928)	785 (104)
	2035 (6)	800 (61)
$(\text{HgH}_2)_3$	1905 (985 × 2)	785 (89 × 2)
	2031 (4 × 2)	792 (87)

<sup>a</sup> Infrared intensities,  $\text{km/mol}$ . <sup>b</sup> Frequencies 1960 and  $802 \text{ cm}^{-1}$  calculated at the CCSD(T) level<sup>6</sup> substantiate the DFT results.

strongest absorption  $12.8 \text{ cm}^{-1}$  lower than the dimer, and we observe the trimer  $10.3 \text{ cm}^{-1}$  lower. These bands show almost the same H/D frequency ratios as  $\text{HgH}_2$  (1.3914, 1.3908, respectively); hence, similar molecules are involved in the vibrational modes. Furthermore, our calculations predict strong and weak bending modes for each cluster in very good agreement with observed values.

Figure 1 reveals a considerable spectroscopic difference for the next larger  $(\text{HgH}_2)_n$  cluster. A weak, broad  $1880\text{--}1800 \text{ cm}^{-1}$  absorption evolves on warming into a  $1836 \text{ cm}^{-1}$  shoulder and a sharper  $1802.0 \text{ cm}^{-1}$  peak in the Hg–H stretching region, and associated bands appear at  $739.1$  and  $672.9 \text{ cm}^{-1}$  in the H–Hg–H bending region. These absorptions are due to a new solid material formed as molecules coalesce first into an amorphous material then into a crystalline molecular solid upon sublimation of the solid  $\text{H}_2$  host. This new solid decomposes in the  $150\text{--}170 \text{ K}$  temperature range, and a solid mercury residue is found on the window at room temperature. The H/D frequency ratios 1.390 and 1.387 of our solid absorptions are again similar to the 1.3901 H/D ratio for the Hg–H stretching mode in  $\text{HgH}_2$ , and the H/D ratios for the bending modes, 1.3898 and 1.3764, are slightly lower than the 1.3902 value determined for  $\text{HgH}_2$ . In addition the two solid HD counterpart absorptions at  $1874$  and  $1339 \text{ cm}^{-1}$  (Figure 3) show almost the same isotopic relationship with the  $1802.0 \text{ cm}^{-1}$  pure  $\text{H}_2$  and  $1299.7 \text{ cm}^{-1}$  pure  $\text{D}_2$  absorptions, namely  $72$  and  $39 \text{ cm}^{-1}$  higher, as found for the strong  $\text{HHgH}$ ,  $\text{HHgD}$ , and  $\text{DHgD}$  isotopic molecule stretching modes, where  $\text{HHgD}$  bond stretching modes are  $54$  and  $30 \text{ cm}^{-1}$  higher than antisymmetric values for  $\text{HgH}_2$  and  $\text{HgD}_2$  (Table 1). This shows that Hg–H vibrational mode coupling is slightly higher in the solid. However, the  $1819 \text{ cm}^{-1}$  band for  $\text{HHgH}$  and the  $1308 \text{ cm}^{-1}$  band for  $\text{DHgD}$  in solid  $\text{HHgD}$  show small differences ( $17$  and  $8 \text{ cm}^{-1}$ ), which evidence weak intermolecular interactions in this molecular solid mercury hydride. Furthermore, the latter  $\text{HHgH}$  and  $\text{DHgD}$  absorption intensities increase with increasing temperature in solid  $\text{HHgD}$  (Figure 3), and the solid structure must be able to readily accommodate H/D exchange.

The above comparisons of HD substitution in the  $\text{HgH}_2$  molecule and solid show that the solid contains  $\text{HgH}_2$  molecules and does not go through  $\text{HHgHgH}$  molecules on decomposition. This conclusion is based on reduced Hg–H stretching mode coupling in  $\text{HHgHgH}$  ( $\text{HHgHgD}$ ) modes at  $1804$  and  $1278 \text{ cm}^{-1}$  in solid HD, which are only  $33$  and  $6 \text{ cm}^{-1}$ , respectively, above  $\text{HHgHgH}$  in solid  $\text{H}_2$  and  $\text{DHgHgD}$

in solid  $\text{D}_2$  (Table 1)), and therefore our solid absorptions are not appropriate for a  $\text{HHgHgH}$  molecular solid.

We interpret the above evidence to indicate that the next cluster  $(\text{HgH}_2)_n$  evolves from dimer and trimer, and our attempts to calculate tetramer structures converge into a coplanar dimer of dimers. We believe solid  $\text{HgH}_2$  incorporates stacked planes of  $\text{HgH}_2$  molecules built on the dimer model, which may be compared to a box of pencils with the pencils tilted by  $35^\circ$ . The sharp  $1802.0 \text{ cm}^{-1}$  absorption probably arises from  $\text{HgH}_2$  submolecules inside of the bulk volume where the  $\text{HgH}_2$  molecule is completely surrounded, and the broad  $1836 \text{ cm}^{-1}$  shoulder from  $\text{HgH}_2$  molecules on the solid surface. Another possibility is that the  $1836 \text{ cm}^{-1}$  band is due to a combination of the  $1802.0 \text{ cm}^{-1}$  fundamental and a  $34 \text{ cm}^{-1}$  lattice mode. Note that the  $1802.0$  and  $672.9 \text{ cm}^{-1}$  bands have similar contours.

## Conclusions

We suggest that a weak mercurophilic  $(\text{Hg(II)}\text{--Hg(II)})$  attraction is responsible for  $(\text{HgH}_2)_n$  clusters in the molecular crystal. This metallophilic interaction has been computed for dimers and assigned a van der Waals radius of  $175 \text{ pm}$  for  $\text{Hg(II)}$  by Pyykkö and Straka.<sup>16</sup> Although metallophilic bonding is not inherently relativistic, it is strengthened considerably by the large relativistic effects for heavy elements such as mercury.<sup>20,22</sup> Some electrostatic interaction involves the hydrogen ligands as the Hg–H stretching mode coupling is slightly higher in the solid based on HD substitution and on the H/D exchange observed in solid  $\text{HHgD}$  on warming.

We find the structure of solid mercury hydride to be very different from that for solid zinc hydride, which has been prepared by a number of routes, and the white solids so formed decompose in the  $90\text{--}115 \text{ }^\circ\text{C}$  range.<sup>23–27</sup> Zinc uses facile  $4s\text{--}4p$  hybridization and forms covalent chains. Solid zinc hydride is presumably an associated hydrogen-bridged polymer like magnesium hydride, and the broad infrared absorptions for zinc hydride ( $1900\text{--}1300$ ,  $1150\text{--}850$ ,  $650\text{--}500 \text{ cm}^{-1}$ )<sup>25,27</sup> are in agreement with this bonding model. On the other hand, mercury hydride solid is much less stable decomposing at  $150\text{--}170 \text{ K}$ , in agreement with the finding of Wiberg and Henle,<sup>9</sup> which we believe is characteristic of a different bonding interaction, namely that of a covalent molecular crystalline solid. Owing to relativistic effects,<sup>22</sup> mercury prefers the linear, predominately  $5d\text{--}6s$  hybridization and two-coordination.<sup>28</sup> We propose that solid mercury hydride consists of rows of  $\text{HgH}_2$  molecules held together mainly by mercurophilic bonding attractions instead of the hydrogen-bridged bonding involved in lighter metal hydride solids.

(22) Pyykkö, P. *Chem. Rev.* **1988**, *88*, 563.

(23) Barbaras, G. D.; Dillard, C.; Finholt, A. E.; Wartik, T.; Wilzbach, K. E.; Schlesinger, H. I. *J. Am. Chem. Soc.* **1951**, *73*, 3, 4585.

(24) Wiberg, E.; Henle, W.; Bauer, R. Z. *Naturforsch.* **1951**, *6b*, 393 (Zn).

(25) De Koning, A. J.; Boersma, J.; van der Kerk, G. J. M. *J. Organomet. Chem.* **1980**, *186*, 159.

(26) Shaw, B. L. *Inorganic Hydrides*; Pergamon: Oxford, U.K., 1967.

(27) Wang, X.; Andrews, L. *J. Phys. Chem. A*, in press.

(28) Orgel, L. E. *J. Chem. Soc.* **1958**, 4186.

In this regard,  $\text{HgH}_2$  is like the more common  $\text{HgCl}_2$ , which forms a van der Waals molecular solid of linear  $\text{HgCl}_2$  molecules.<sup>1</sup> The  $\text{HgCl}_2$  molecule is linear in the gas phase,<sup>29,30</sup> and the antisymmetric stretching fundamental red shifts only  $6\text{ cm}^{-1}$  to  $407\text{ cm}^{-1}$  on isolation in a krypton matrix.<sup>31</sup> However, in the van der Waals solid this mode shifts further to about  $375\text{ cm}^{-1}$  (see ref 31), a displacement of 7.9%. Our  $\text{HgH}_2$  antisymmetric stretching fundamental sustains a 5.3% shift from the molecule isolated in a hydrogen matrix to the

molecular solid, and  $\text{HgD}_2$  shifts 5.0% from the deuterium matrix to the solid  $\text{HgD}_2$  value. Hence, the volatile molecular solid  $\text{HgH}_2$  formed here is similar to the higher molecular weight van der Waals solid  $\text{HgCl}_2$ .

**Acknowledgment.** This work was supported by the National Science Foundation (Grant CHE 00-78836). We acknowledge helpful correspondence with P. Pyykkö.

IC049100M

---

(29) Balabanov, N. B.; Peterson, K. A. *J. Chem. Phys.* **2003**, *119*, 12271 and references therein.

(30) Büchler, A.; Stauffer, J. L.; Klemperer, W. *J. Am. Chem. Soc.* **1964**, *86*, 4544.

---

(31) Lowenschuss, A.; Ron, A.; Schnepf, O. *J. Chem. Phys.* **1969**, *50*, 2502 and references therein.